Interfacial Velocities in the Vicinity of a Sieve Plate Sparger

Larry A. Glasgow and Robert Rainbolt
Dept. of Chemical Engineering, Kansas State University, Manhattan, KS 66506

In a recent article, Rainbolt and Glasgow (1993) described bubble formation transitions observed at a sieve plate sparger in a laboratory-scale airlift reactor. These transitions included both bubbling mode and active hole location; they were particularly energetic at moderate superficial gas velocities. A component of this study concerned evaluation of the fluid motions accompanying bubble formation with efforts directed at identifying the origins of strain rates that might produce cellular damage in culture operations. While this previous work gave some indications that energetic fluid motions might be driven by interfacial phenomena near the point of bubble formation, standard tools used to quantify fluid motion like laser-Doppler velocimetry were not at all conclusive. We have now completed an extensive study of the initial rise of bubbles following detachment from sieve plate spargers using high-speed videography and have observed previously unquantified phenomena that result in very energetic fluid motions.

Hughes et al. (1955) studied bubble formation at simple orifices describing their three regimes: very low flow rates where bubble volume is virtually constant; intermediate rates where bubble size depends on flow; and high gas rates where the gas jet is broken into bubbles. They described the results of a dimensional analysis of the bubble formation process, indicating that bubble volume depended on a Reynolds number, defined as:

$$Re = q\rho_L/(\pi d\mu_L) \tag{1}$$

where q is the volumetric flow rate through the orifice, and a surface tension number,

$$N_\sigma = \sigma\rho_L d_o/\mu_L^2 \tag{2}$$

where d_o is the orifice diameter. They also carefully pointed out the importance of the gas chamber (train) volume with respect to the bubble formation process; their data made it clear that gas chamber volume has a pronounced effect on bubble volume, particularly at lower frequencies of formation where small chamber volumes resulted in small bubbles.

This work focuses on local interfacial velocities associated with the bubble phenomena occurring immediately after detachment above sieve plate spargers. We have done this because it is apparent from the literature that no completely definitive data have appeared regarding the origins of energetic fluid motions leading to loss of cellular viability in culture operations. For example, Tramper et al. (1987) found most of the damage occurring to suspended insect cells happened in the immediate vicinity of the point of air injection with the death rate inversely related to bubble size. Lu et al. (1992), on the other hand, studied the effects of interfacial phenomena and fluid motions on the integrity of nylon microcapsules (the 50% cumulative volume corresponded to a size of 180 to 200 μm). They concluded that in bubble column operation, bubble disengagement (bursting) was the principal cause of microcapsule breakage. And Handa-Corrigan et al. (1989) attributed cell damage occurring in the culture of suspended mammalian cells to interfacial phenomena associated with bubble disengagement and film drainage in foams.

Experimental Details

All of the work described here was conducted in an acrylic plastic airlift reactor with a volumetric capacity of 3 L. A very detailed description of this apparatus has been provided in our earlier article and will not be repeated here. Air bubbles were generated in this apparatus with interchangeable sieve plate spargers; the one used principally in this work had five 1.1-mm holes. Liquid media employed included distilled water and aqueous solutions of 48% and 72% glycerol. The 48% glycerol solution had a viscosity (μ) of 5 cp and a surface tension (σ) of 70 dyne/cm; for the 72% solution, $\mu = 17$ cp and $\sigma = 68$ dyne/cm. The surface tension numbers, N_σ, were 7,920, 345, and 31 for distilled water, 48% glycerol, and 72% glycerol, respectively. The gas rates employed in this investigation provided superficial air velocities ranging from about 0.1 to 0.7 cm/s, based on the cross-sectional area of the upflow side of the reactor. The use of this range of gas velocities ensured that only one sieve-plate hole would be actively bubbling. Throughout this investigation, the airlift reactor was operated as a bubble column without circulation about the divider. We also operated with maximum gas chamber volume such that the region under the sieve plate was completely occupied by gas.

Bubble behaviors were observed and recorded with a Kodak Ektapro high-speed video system at 1,000 frames per second; attention was focused on the ~2 cm immediately above the sieve plate. An Olympus 50-mm macrolens was employed, and the useful digital video frames were replayed as an NTSC signal and recorded with a Sony 8-mm VTR for later playback and analysis. The monitor images were about nine times larger than actual entity size. Data obtained from the video record included bubble size and shape, and the vertical velocity of both the upper and lower bubble interfaces; the velocities were obtained by observation of the number of frames required for the appropriate surface to pass through the 2-cm field of view. Extensive experience indicated that the likely error was about ±1 frame at both the top and bottom of the appropriate video sequence. At an interfacial velocity of 35 cm/s, this would correspond to a worst-case error in the velocity determination of about 3.5%. The data reduction process was completely manual and could best be described as tedious. Distributions for bubble interface velocities were obtained from ensembles typically consisting of 150 to 300 bubble observations. To assess the reproducibility of this process, preliminary trials were carried out in which the upper bubble surface velocity was measured for four separate sets of 180 bubbles, each in 50% glycerol with a superficial gas velocity, U_g, of about 0.55 cm/s. The resulting distributions appear in Figure 1 plotted as discrete points; the solid line is the composite distribution for the entire collection of 720 observations. Note that the very same features appear in all of the distributions and that the maxima are similarly located in each set. Because aspects of the bubble formation process are inherently chaotic, one cannot expect these ensemble determinations to yield identical results.

At very low gas velocities, $U_g \leq 0.3$ cm/s, bubble formation in our apparatus occurs in intermittent groups; in this mode, a sequence of four to six bubbles is followed by a period of inactivity. Furthermore, the volumetric flow rate through the orifice generally decreases during the formation sequence. Repeated analysis of this behavior for the air-water system with $U_g = 0.22$ cm/s indicated that the initial volumetric flow rate was approximately 19 cm^3/s. At the midpoint of the bubble formation sequence, the flow rate was usually on the order of 10 to 11 cm^3/s; at the time of formation of the last bubble in the train, the flow rate was often between 5 and 6 cm^3/s. This means that for the intermediate (sequence) flow rates in the air-water system, the bubble Reynolds number (as given by Eq. 1) was generally about 400 for bubble diameters of about 8 to 10 mm. Qualitatively similar behavior was observed in the glycerol system, with bubble trains consisting of four to six bubbles being formed intermittently for $U_g \leq 0.25$ cm/s. In fact, at $U_g \cong 0.08$ cm/s, about 57 clusters were formed per minute and at $U_g \cong 0.2$ cm/s, nearly 150 episodes of sequential bubble formation occurred per minute. Ultimately, however, phenomena accompanying somewhat larger superficial gas velocities proved to be of greater interest.

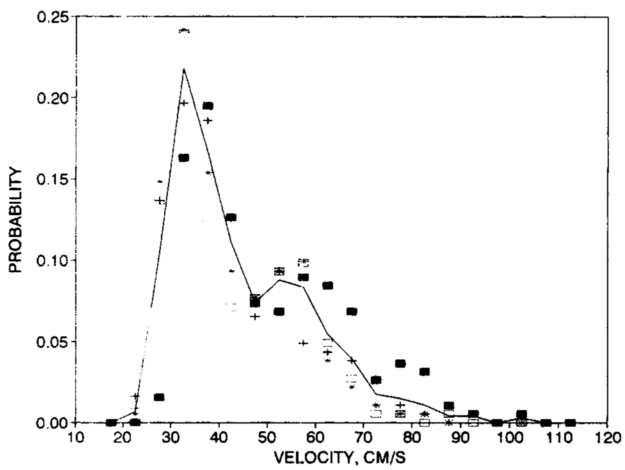

Figure 1. Assessment of reproducibility of interfacial (bubble top) velocity determinations: four separate sets of 180 observations each were processed for 50% glycerol with $U_g \approx 0.55$ cm/s.

The composite distribution for the entire sample is shown as a solid line.

Results

We concentrated initially upon the movement of the upper surface of air bubbles in distilled water through ~2 cm immediately above the sieve plate following detachment. It became apparent at once that buoyancy and drag were not the only forces affecting bubble movement in this area. The proximity of the preceding bubble was a key factor in determining bubble-top velocity; in some cases, trailing bubbles caught and coalesced with preceding bubbles. When this occurred, the trailing bubble was often highly elongated vertically. Data from this segment of the investigation are shown in Figure 2 for U_g's ranging from 0.26 to 0.59 cm/s; the results are presented as frequency or probability of occurrence over the range of detected velocities. In all cases for the air-water system, the maximum probability occurred at about 32 cm/s. However, three of the distributions show secondary maxima; these features are located between 47 and 55 cm/s. And two of the curves exhibit relatively small probabilities at 90 to 100 cm/s resulting from the capture-coalescence phenomena described above.

Data obtained with 48% and 72% glycerol are much different than those described above for distilled water; in the

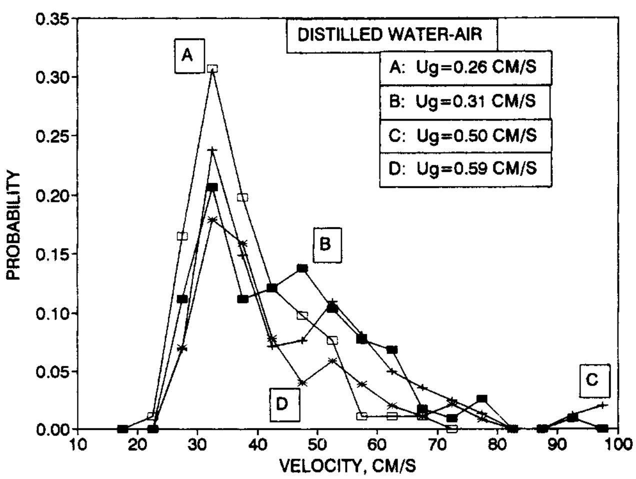

Figure 2. Frequency of occurrence for bubble top (upper interface) velocities in distilled water.

Velocities were measured over 2 cm immediately above sieve plate sparger.

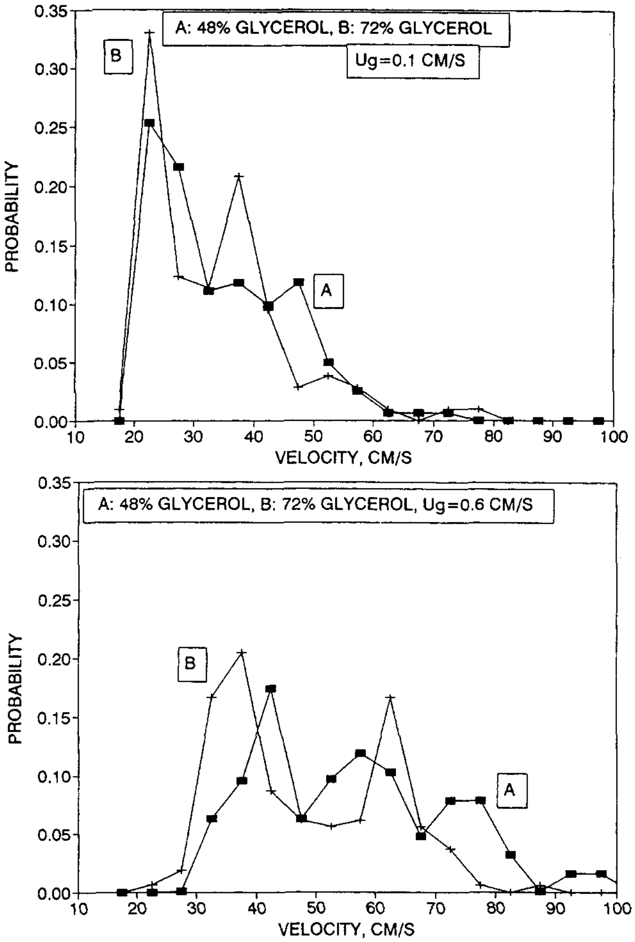

Figure 3. Frequency of occurrence for bubble top (upper interface) velocities in aqueous glycerol solutions: upper half, $U_g \approx 0.1$ cm/s and lower half, $U_g \approx 0.6$ cm/s.

Velocities were measured over 2 cm immediately above sieve plate sparger.

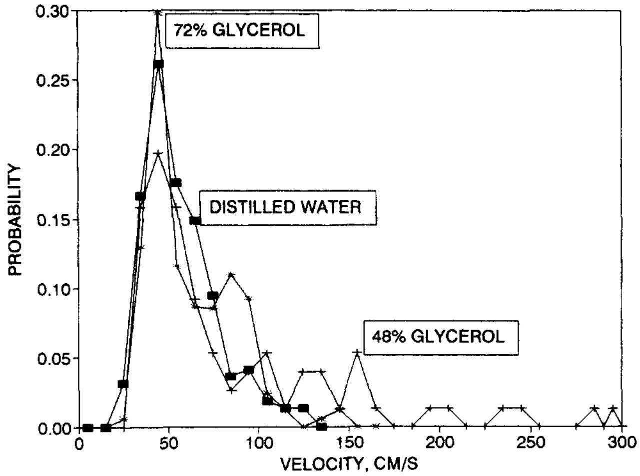

Figure 4. Frequency of occurrence for bubble bottom (lower interface) velocities in distilled water and 48 and 72% aqueous glycerol solutions with $U_g \approx 0.6$ cm/s.

Velocities were measured over 2 cm immediately above sieve plate sparger.

glycerol solutions, the distribution of bubble-top velocities is clearly affected by both viscosity and gas flow rate. Figure 3 shows bubble-top velocities in 48% and 72% glycerol for U_g's of approximately 0.1 (upper half) and 0.6 cm/s (lower half). The maximum probability for each distribution is uniquely located; the maxima occur at 21 and 44 cm/s in 48% glycerol for the superficial gas velocities cited, respectively. Furthermore, the higher gas rates clearly produce upper bubble interface motions with significant probability of occurrence at 50 to 100 cm/s, despite the viscosities of 5 and 17 cp. For $U_g \cong 0.6$ cm/s in particular, a substantial region of probability is found in the range of 60 to 80 cm/s.

The data obtained regarding the motion of upper bubble surfaces immediately above a sieve plate sparger are interesting, but the velocities of the bottom bubble interface under certain conditions are extraordinary. Figure 4 shows a comparison of lower interface (bubble bottom) velocities immediately following bubble detachment in distilled water, 48% glycerol, and 72% glycerol at U_g of 0.6 cm/s; this provides a clear indication of the effects of viscosity on the motion of the lower bubble interface. Note that for the air-water system, the maximum probability occurs at 44 cm/s, and a significant number of events yield velocities around 90 to 120 cm/s. These latter occurrences are being driven by capture-coalescence where the trailing end of a highly-elongated structure is retracted *very* rapidly. In the 48% glycerol solution, the maximum probability is also located at about 44 cm/s, but a significant number of events involve velocities at 150, 200, 240 and about 290 cm/s. It is important to note that the reported velocities are average values determined over the entire ~2 cm field of view; frame-by-frame analysis of bubble (bottom interface) motions in 48% glycerol reveals instantaneous velocities in excess of 300 to 350 cm/s. This phenomenon appears to be most pronounced at intermediate viscosity, at least at the upper end of the superficial gas velocities considered here. For 48% glycerol with $U_g \cong 0.6$ cm/s, these very energetic lower interface retraction events occur more often than five times per second in our apparatus. In 72% glycerol, no bottom interface velocities larger than 150 cm/s were observed at any superficial gas velocity.

The liquids employed in this investigation are low Morton number systems, where

$$Mo = g\mu_L^4/(\rho_L \sigma^3) \tag{3}$$

In fact, 48% glycerol gives $Mo = 1.6 \times 10^{-8}$, which means that air bubbles in this system can be expected to exhibit oscillation in the bubble rise path if $We \geq 2$ to 3. In the case of this work, the ultimate bubble pathway is not recorded since the high-speed video system is focused on the region immediately above the sieve plate; however, Weber numbers can be determined based on the bubble velocities and sizes apparent in this limited region:

$$We = \rho_L u_b^2 d_e/\sigma, \tag{4}$$

where u_b is the rise velocity of the upper bubble interface over the frame of observation, and d_e is the equivalent bubble diameter. Weber numbers were determined for the 48% and 72% glycerol systems; the superficial gas velocities were about 0.1 cm/s and about 0.6 cm/s. Most *We* values lie in the range of 4 to 10 for 48% glycerol at $U_g \cong 0.1$ cm/s, although there is also a significant concentration of *We* between 20 and 30 in this system. It is certain that these data are being skewed by bubble capture-coalescence events resulting in aberrantly large bubble velocities. For 72% glycerol at $U_g \cong 0.6$ cm/s, the values of *We* are inflated by the larger gas velocity, resulting in many *We* in the range of 40 to 60. In the 48% glycerol case with $U_g \cong 0.6$ cm/s, the frequent capture-coalescence events lead to significant numbers of *We* in the range of 70 to 100. For comparison, we note that in the air-water system at a superficial gas velocity of about 0.3 cm/s, nearly 79% of the measured Weber numbers are between 5 and 20, and only 12% of *We* are larger than 25.

Conclusions

We find that air bubbles leaving a sieve plate sparger from a single hole in both distilled water and aqueous glycerol solutions will occasionally overtake preceding bubbles, possibly culminating in capture and coalescence. When this occurs, the bottom surface of the elongated trailing bubble may be retracted very rapidly, producing local instantaneous interfacial velocities in 48% glycerol that *exceed* 300 cm/s. This effect appears to be particularly common in fluids of medium viscosity at the upper end of the range of superficial gas velocities employed. It does not seem to occur when the vertical space between successive bubbles exceeds about 8 or 9 mm. The most significant finding is that interfacial motions occurring near the point of bubble origin due to capture-coalescence may rival in violence those accompanying bubble disengagement processes; under some circumstances in our apparatus, the phenomenon of abrupt lower interface retraction occurs more often than five times per second for bubbles emanating from a single sieve plate hole.

Acknowledgment

This material is based on work supported in part by NSF-EPSCoR Grant No. OSR-9255223 and the Government has certain rights in this material. The State of Kansas also provided partial support for this work.

Literature Cited

Handa-Corrigan, A., A. N. Emery, and R. E. Spier, "Effect of Gas-Liquid Interfaces on the Growth of Suspended Mammalian Cells: Mechanisms of Cell Damage by Bubbles," *Enzyme Microb. Tech.*, **11**, 230 (1989).

Hughes, R. R., A. E. Handlos, H. D. Evans, and R. L. Maycock, "The Formation of Bubbles at Simple Orifices," *Chem. Eng. Prog.*, **51**, 557 (1955).

Lu, G. Z., B. G. Thompson, and M. R. Gray, "Physical Modeling of Animal Cell Damage by Hydrodynamic Forces in Suspension Cultures," *Biotech. and Bioeng.*, **40**, 1277 (1992).

Rainbolt, R., and L. A. Glasgow, "An Experimental Study of Bubble Formation Transitions at Sieve Plate Spargers," *Chem. Eng. Comm.*, **119**, in press (1993).

Manuscript received Mar. 22, 1993, and revision received June 3, 1993.